

Optimal (Bandpass) Continuous-Time $\Sigma\Delta$ Modulator

Omid Shoaee and W. Martin Snelgrove
 Department of Electronics, Carleton University
 Ottawa, Ontario, Canada K1S 5B6
 1-613-788-2381
 omid@doc.carleton.ca & snelgar@doe.carleton.ca

ABSTRACT

A systematic technique for designing a continuous-time sigma-delta modulator ($\Sigma\Delta$) is presented. The continuous-time $\Sigma\Delta$ open-loop transfer function is obtained by the pulse-invariant transformation of its discrete-time equivalent. This method results in an inherently stable $\Sigma\Delta$ and does not need any loss factor to make the modulator stable, and so provides the maximum achievable signal-to-noise ratio. Properties of the continuous-time $\Sigma\Delta$ are described. The technique has been applied to conventional lowpass and bandpass $\Sigma\Delta$ s, and a general fourth-order bandpass example is given to illustrate the theory.

I. INTRODUCTION

It is often desirable to convert a bandpass analog signal to digital as near the front end of the receiver as possible in digital receiver systems. Baseband sigma-delta analog to digital (A/D) converters have been extensively used in audio band frequencies [1] where the $\Sigma\Delta$ loop filter is usually implemented by integrators. Since it's intuitively reasonable that replacing "integrators" with "resonators" should make a bandpass converter, several researchers have looked at using switched-capacitor (SC) resonators [2] and LC [3]-[5] in $\Sigma\Delta$ loops. A 4th-order bandpass $\Sigma\Delta$ modulator architecture including two series resonators was implemented in a switched-capacitor (SC) technology [2].

Continuous-time modulators can be far faster than their SC counterparts, and contain implicit anti-alias filtering. The sample-and-hold is not as serious a concern since it can be placed after several resonators and thus errors due to imperfect sampling will be noise-shaped. It is, however, difficult to construct linear high-Q resonators on-chip, so these converters have generally relied on off-chip inductors.

Early designs were approximate, guided by the intuition that resonators should work, and had to spoil the Q of their resonators to make fourth-order bandpass modulators stable, which reduced the effectiveness of noise shaping. In [3],[5] for example, a damping resistor is placed in parallel with LC circuit(s) to stabilize the $\Sigma\Delta$ loop, but causes the fourth-order $\Sigma\Delta$ to behave more or less as a second-order system. This turns out to be unnecessary, because the noise-

shaping behavior of "continuous-time" $\Sigma\Delta$ loops can be designed entirely in the discrete-time domain and the exact same noise-shaping behavior obtained for either continuous-time or discrete-time "resonators". This happens because the loop behavior is completely determined by what the sampler inside the loop (the quantizer is clocked, making for implicit sampling) sees at its sample times, and that can be written as a difference equation. Therefore the loop transfer function in continuous-time $\Sigma\Delta$ has an exact equivalent Z-domain transfer function.

II. TRANSFORMATION OF DISCRETE-TIME $\Sigma\Delta$ TO CONTINUOUS-TIME $\Sigma\Delta$

As a simple example, look at the first-order lowpass modulator in Fig. 1, where continuous-time signals are distinguished with "hats" and the "zero-order hold" function converts a sample stream to a non-return-to-zero (NRZ pulse) waveform. Its equations can be written by inspection:

$$y(k) = \text{sgn } u(k) = \text{sgn } \hat{u}(kT) \quad (1)$$

and

$$\begin{aligned} u(k+1) &= \hat{u}([k+1]T) \\ &= \hat{u}(kT) + \frac{1}{\tau} \int_{kT}^{(k+1)T} (\hat{x}(t) - y(k)) dt \end{aligned}$$

which is a difference equation as far as $u(k)$ is concerned:

$$u(k+1) = u(k) - \frac{T}{\tau} y(k) + \frac{1}{\tau} \int_{kT}^{(k+1)T} \hat{x}(t) dt \quad (2)$$

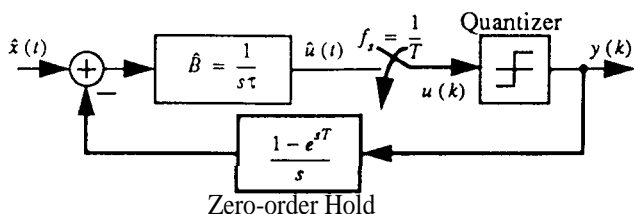


Fig. 1: A first-order continuous-time $\Sigma\Delta$ loop.

Equations (1) and (2) describe (exactly!) a first-order $\Sigma\Delta$ loop with a feedback gain T/τ and an input signal that is

prefiltered by a boxcar integration (hence the comment above that there is “implicit anti-alias filtering”).

This is generalized [4] using an impulse-invariant transformation, which converts term-by-term between the partial-fraction expansion of a discrete-time response $B(z)$ and a continuous-time $\hat{B}(s)(1-e^{-sT})/s$. Working with the partial-fraction expansion (the first step of inverting the Laplace transform) is the way to guarantee that the impulse responses are equal at sample times kT , and the $(1-e^{-sT})/s$ term accounts for the zero-order hold at the D/A feedback to the continuous-time integrator. Writing the continuous-time loop filter as

$$\hat{B}(s) = \sum_{k=1}^N \frac{\hat{b}_k}{s-s_k} \quad (3)$$

an equivalent discrete-time system has loop filter

$$B(z) = \sum_{k=1}^N \frac{b_k}{z-z_k} \quad (4)$$

where the new residue is

$$b_k = \frac{b_k}{-s_k} (1 - e^{s_k T}) \quad (5)$$

and the new pole is at

$$z_k = e^{s_k T} \quad (6)$$

This has the properties one would expect: a pole at $s=0$ transforms to one at $z=1$, and one at $s=j2\pi(f_s/4)$ transforms to $z=j$.

Applying (5) to the first-order case with $\hat{B}(s)=1/s$ gives an unfortunate cancellation: $b_k=(1/0)(1-e^{0T})=0/0$, but the ambiguity is easily resolved either by using L'Hôpital's rule or by taking a limit of (5) as $s_k \rightarrow 0$. Looking at an expansion of $e^{s_k T}$:

$$b_k = \frac{b_k}{-s_k} (1 - e^{s_k T}) = \frac{b_k}{-s_k} (1 - (1 + s_k T + \dots))$$

shows that for poles at DC

$$s_k = 0 \Rightarrow b_k = \hat{b}_k T \quad (7)$$

Which gives the form that we found in the special case that derived (2).

Equation (5) gives a simple translation that lets a designer take an arbitrary $B(z)$, rewrite it in the form of (4), and get an $\hat{B}(s)$ that gives an exactly equivalent loop. That's enough to design continuous-time bandpass (or lowpass, for that matter) $\Sigma\Delta$ converters, except for a couple of ‘fine points’: (4) can't handle multiple poles (such as you find in a conventional second-order $\Sigma\Delta$ or its bandpass version); and high-linearity feedback DACs use return-to-zero waveforms rather than NRZ. Now we'll correct these problems.

Repeated poles in a rational function produce additional terms (besides those in (4)) in the partial fraction expansion, which have the form

$$\frac{b'_k}{(z-z_k)^2} \quad (8)$$

The poles move to points s_k with $e^{s_k T} = z_k$, just as before, and the corresponding term in the continuous-time equivalent becomes

$$b'_k \frac{(1-s_k T - e^{-s_k T})}{(1-e^{s_k T})^2} \frac{s}{T} + \frac{s^2}{(1-e^{s_k T})^2} \quad (9)$$

which has repeated poles, just as in the Z-domain, but has a numerator with both bandpass (s) and lowpass (constant) terms. From (5) and (9) it could easily be shown that a conventional second-order $\Sigma\Delta$ with $B(z)=(z-1)/(z-1)^2$ has a continuous-time equivalent with $\hat{B}(s)=(1+1.5sT)/s^2 T^2$ (already known [6]). For a complex pole the numerator in (9) has complex coefficients, but a conjugate term $\bar{b}'_k/(z-\bar{z}_k)$ produces a conjugate numerator term.

The particularly important case $B(z)=(2z^2+1)/(z^2+1)^2$ (which gives the fourth-order bandpass converter of [7], for example) produces a fourth-order filter with a third-order numerator and a double pole at $1/(4T)=f_s/4$

$$\hat{B}(s) = \frac{\left(\frac{\pi}{2} - \frac{1}{4}\right) \frac{s^3}{T} + \left(\frac{3\pi^2}{16} + \frac{\pi}{4}\right) \frac{s^2}{T^2} + \left(\frac{\pi^3}{8} + \frac{\pi^2}{16}\right) \frac{s}{T^3} + \frac{3}{4} \left(\frac{\pi}{2T}\right)^4}{\left(s^2 + \left(\frac{\pi}{2T}\right)^2\right)^2} \quad (10)$$

The simple way to build a double pole, in continuous time, is with a pair of bandpass resonators [3], but that approach gives a numerator with only an s^2 term, which doesn't give the right $\hat{B}(s)$. We will show an appropriate structure in section III to realize the preceding transfer function.

A second generalization of (5) is needed to allow the use of return-to-zero DAC waveforms like the one shown in Fig. 2, which reduce the nonlinearity due to the fact that the area under a practical pulse depends on the levels of the preceding and following pulses. The effect this has is to replace the zero-order hold $(1-e^{-sT})/s$ with a half-sample hold

$$\frac{1 - e^{-sT/2}}{s} \quad (11)$$

which just would make a straightforward change in (5)

$$b_k = \frac{b_k}{-s_k} (1 - e^{s_k T/2}) e^{s_k T/2} \quad (12)$$

III. A FOURTH-ORDER EXAMPLE

3.1. TRANSFER FUNCTION DESIGN

A discrete-time modulator could be expressed with a configuration shown in Fig. 3 [2] in which $A(z)$ and $B(z)$ represent feedforward and loop transfer function respectively. Correspondingly, Fig. 4 shows the equivalent structure for a continuous-time modulator. $B(z)$ is usually selected among

the conventional $\Sigma\Delta$ transfer functions or is optimized by any optimization tools to achieve the required noise transfer function (NTF). However, $A(z)$ is obtained based on $B(z)$ to meet the signal transfer function (STF) specifications, usually 0dB gain inside the band and infinite attenuation in band-reject regions.

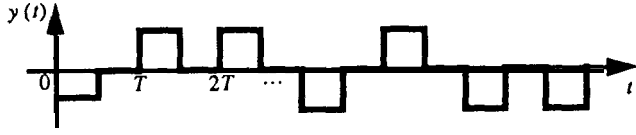


Fig. 2: Return-to-zero DAC waveforms reduce nonlinearity from memory effects.

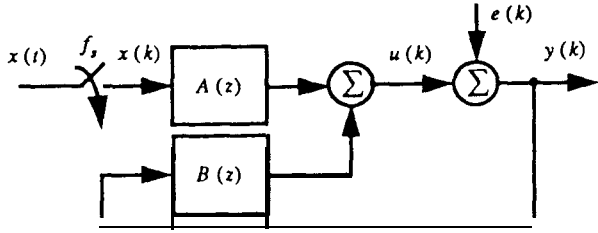


Fig. 3: Discrete-time sigma-delta modulator (A and B transfer functions share poles).

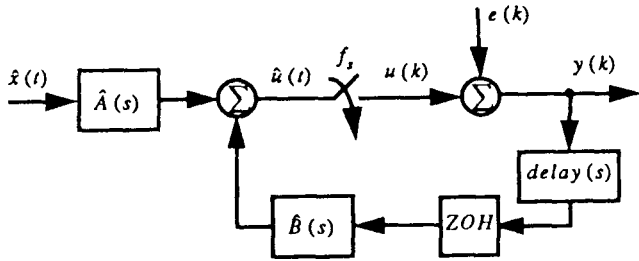


Fig. 4: Continuous-time $\Sigma\Delta$ modulator, equivalent to the discrete-time modulator shown in Fig. 3.

3.1.1. multiple-pole design

The loop transfer function $\hat{B}(s)$ is given by eqn. (10) which was obtained from the discrete equivalent transfer function $B(z) = (2z^2 + 1)/(z^2 + 1)$. It can easily be shown that $A(z) = 0.5z(z^2 - 1)/(z^2 + 1)^2$ provides a flat response inside the band and zeros at DC and $f_s/2$ for discrete-time STF. The corresponding continuous-time feedforward transfer function $\hat{A}(s)$ would be

$$\hat{A}(s) = 0.25 \frac{\left(\frac{\pi}{2} - 1\right) \frac{s^3}{T} - \pi \frac{s^2}{T^2} + \left(\frac{\pi}{2} + 1\right) \left(\frac{\pi}{2}\right)^2 \frac{s}{T^3}}{\left(s^2 + \left(\frac{\pi}{2T}\right)^2\right)^2} \quad (13)$$

which along with $\hat{B}(s)$ provides an implicit bandpass anti-alias filtering for the continuous-time $\Sigma\Delta M$ (zero at $s=0$ in eqn. (13)).

3.1.2. spread-pole design

The NTF and STF for a 4th order bandpass example (with center frequency at 20MHz and bandwidth of 1MHz) have

been optimized by “fitorX”[8]. The NTF zeros turn out to be at $z = \exp(\pm \pi/2 \pm 0.02527)j$ $j = \pm 0.025268 \pm 0.999681j$ and poles at $z = i0.33447 \pm 0.69822j$.

The corresponding S-domain loop transfer function ($\hat{B}(s)$) and feedforward transfer function ($\hat{A}(s)$) obtained by pulse invariant transformation given in (3)-(6) are

$$\hat{B}(s) = \left(\frac{b_3}{T}s^3 + \frac{b_2}{T^2}s^2 + \frac{b_1}{T^3}s + \frac{b_0}{T^4}\right) / \left((s^2 + \omega_1^2)(s^2 + \omega_2^2)\right) \quad (14)$$

and

$$\hat{A}(s) = \left(\frac{a_3}{T}s^3 + \frac{a_2}{T^2}s^2 + \frac{a_1}{T^3}s + \frac{a_0}{T^4}\right) / \left((s^2 + \omega_1^2)(s^2 + \omega_2^2)\right) \quad (15)$$

where $f_s = 1/T = 4f_o = 80\text{MHz}$, $(b_3, b_2, b_1, b_0) = (0.8276, 1.6396, 2.7885, 2.8722)$, $(a_3, a_2, a_1, a_0) = (0.0867, 0.4770, 0.9630, 0.0)$ and $(\omega_1, \omega_2) = ((\pi/2 - 0.02527)/T, (\pi/2 - 0.02527)/T)$.

3.2. GM-C IMPLEMENTATION

The cascade of resonators structure including Transconductor-C (Gm -C) integrators has been chosen for the bandpass modulator. Fig. 5 shows a fourth order bandpass structure including two Gm -C resonators. The transconductors represented by $(g_{m_{a0}}, g_{m_{a1}}, g_{m_{a2}}, g_{m_{a3}})$ and $(g_{m_{b0}}, g_{m_{b1}}, g_{m_{b2}}, g_{m_{b3}})$ implement the zeros and the transconductors represented by $(g_{m_{x1}}, g_{m_{f1}})$ and $(g_{m_{x2}}, g_{m_{f2}})$ implement the common poles of $\hat{A}(s)$ and $\hat{B}(s)$ respectively.

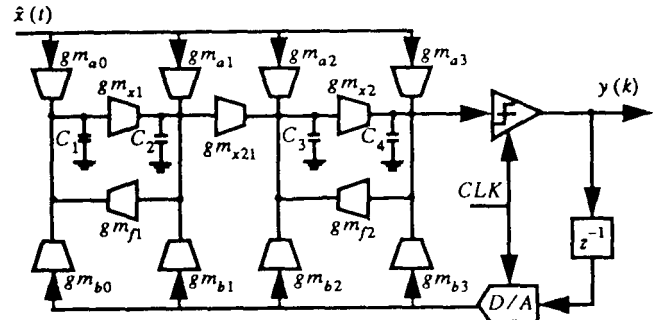


Fig. 5: The 4th-order $\Sigma\Delta Gm$ -C modulator (including cascade of two resonators).

3.3. SIGNAL-TO-NOISE RATIO ($f_{in}=20\text{MHz}$, $BW=1\text{MHz}$)

3.3.1. spread-pole

The ideal Z- and S-domain modulators have been simulated with [JELDO] (v.4.1.x, ANACAD manual). SNRs of the ideal discrete- and continuous-time modulators, for a sinusoidal input of -6 dB, were 62.58 dB and 60.51 dB respectively. The ideal Gm -C circuit shown in Fig. 5, representing the transfer functions given in eqns. (14) and (15), was simulated in ELDO. Fig. 6 shows the bit stream spectrum of the Gm -C modulator, for what the SNR was 59.87 dB,

3.3.2. multiple-pole

The simulated SNR of the ideal multiple-pole discrete-time

modulator was 55.25dB. The corresponding SNRs of the ideal and Gm-C multiple-pole continuous-time modulators with transfer functions given in (10) and (13) were 56.25dB and 55.11dB respectively. As expected the spread-pole design results in higher SNR (almost 5dB in this example).

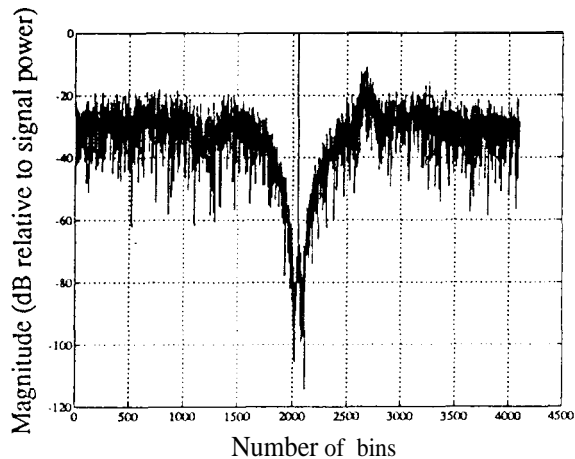


Fig. 6: The bit stream spectrum of simulated 4th order $\Sigma\Delta M$ ($f = 20\text{MHz}$).

3.4. SENSITIVITY TO THE LOOP FILTER PARAMETERS (Q AND RESONANT FREQUENCIES)

A plot of the SNR loss against resonator Q is shown in Fig. 7. For Q of less than 30 idle channel tones started to appear and for Q of less than 20 the noise shaping degraded significantly. From Q=30 to Q=50 the SNR improved by 3dB for each Q increment of 10. From Q=50 to Q=60, the SNR improvement was just 0.4dB and the SNR loss at Q=60 was 2dB. Obviously, at Q of infinity the SNR loss is 0dB.

The SNR is much more sensitive to the resonant frequencies. For spread-pole case, the Gm-C simulations show that shifting both ω_1 and ω_2 ($\omega_1 < \omega_2$) out-of-band by 1% ($(\omega_1 - 0.01\omega_1) \leftarrow \omega_1, \omega_2 \rightarrow (\omega_2 + 0.01\omega_2)$) causes a 10dB SNR loss but when ω_1 and ω_2 are shifted both symmetrically inside the band, the SNR loss is much less. For example, when ω_1 and ω_2 are interchanged *i.e.* $\omega_1 \rightarrow \omega_2$ and $\omega_2 \leftarrow \omega_1$ (3.3% frequency change, in this example), the SNR loss is around 4.5dB. This implies that because of inaccuracy of tuning algorithms it is always better to deliberately shift the resonant frequencies slightly inward in the band in spread-pole design. In this example this would be around 0.8% ($(\omega_1 + 0.008\omega_1) \leftarrow \omega_1$ and $(\omega_2 - 0.008\omega_2) \leftarrow \omega_2$), which cause? 4dB SNR loss, but makes the system less sensitive to resonant frequency changes.

IV. CONCLUSION

The design of a continuous-time bandpass (or lowpass) $\Sigma\Delta$ modulator has been discussed. It has been shown that the pulse invariant transformation is the optimum transformation to preserve the time domain response of a continuous-time $\Sigma\Delta$ modulator loop as that of the discrete-time $\Sigma\Delta M$

equivalent. It has been shown that the continuous-time $\Sigma\Delta$ modulator contains an implicit anti-alias filtering in comparison to the discrete-time (SC) modulator, which is a significant advantage for bandpass A/D conversion.

A Gm-C circuit structure has been introduced and simulated, achieving the expected noise shaping characteristic of $\Sigma\Delta$ modulator while building the anti-alias prefilter.

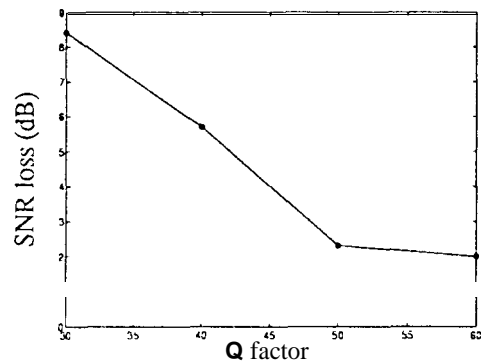


Fig. 7: SNR loss versus Q of resonators.

REFERENCES

- [1] B. P. Del Signore, D. A. Kerth, N. S. Sooch and E. I. Swanson, "A monolithic 20-b delta-sigma A/D converter" *IEEE J. Solid-State Circuits*, vol. 25, No. 6, pp. 1311-1317, Dec. 1990.
- [2] S. Jantzi, W. M. Snelgrove and P. Ferguson, Jr., "A fourth-order bandpass sigma-delta modulator" *IEEE J. Solid-State Circuits*, vol. 28, No. 3 March 1993.
- [3] Gailus et al, "Method and arrangement for a sigma delta converter for bandpass signals" *United States Patent* patent No. 4,857,928. Aug. 1989.
- [4] A. M. Thurston, T. H. Pearce and M. J. Hawksford, "Bandpass Implementation of the Sigma-Delta A-D Conversion Technique," *Proceedings of the IEE International Conference on Analogue-to-Digital and Digital-to-Analogue Conversion*, Swansea, U.K., pp. 81-86, 17-19 Sept. 1991.
- [5] G. Troster, H. J. Drepler, H. J. Golberg, W. Schardein, E. Zocher, A. Wedel, K. Schoppa and J. Arndt, "An interpolative bandpass converter on a 1.2- μm BiCMOS analog/digital array" *IEEE J. Solid-State Circuits*, vol. 28, No. 4, pp. 471-476, Apr. 1993.
- [6] J. C. Candy, "A use of double integration in sigma delta modulation" *IEEE Trans. Commun.*, vol. com-33., No. 3, pp. 249-258, March 1985.
- [7] L. Longo and B. R. Horng, "A 15b 30kHz bandpass sigma-delta modulator" in *Proc. IEEE Int. Solid-State Circuits Conf.*, pp. 226-227, Feb. 1993.
- [8] C. Ouslis, W. M. Snelgrove and A. S. Sedra, "filterX: An interactive design language for filters," *Advances in Electrical Engineering Software, Proceedings of the First International Conference on Electrical Engineering Analysis and Design*, pp. 227-240, Computational Mechanics/Springer Verlag, Aug. 1990.